Expressions for the conductivity and Hall coefficient in the framework of the effective-relaxation-time multidimensional conduction model

H. TIJANI, S. MESSAADI, C. R. PICHARD, A. J. TOSSER
Laboratoire d'Electronique, Université de Nancy 1, BP 239, 54506 Vandoeuvre-les-Nancy Cedex, France

An effective-relaxation-time is used for representing the effects of electronic scattering in thin metallic films from sources other than grain boundaries; the total conductivity of the film is then expressed in terms of the product of an alternative Fuchs–Sondheimer function with an effective grain-boundary multidimensional function. The reduced Hall coefficient is then obtained in the form of the product of the reduced Fuchs–Sondheimer Hall coefficient with an effective reduced grain-boundary Hall coefficient. Qualitative agreement with experimental data is obtained.

1. Introduction

An effective-relaxation-time model [1] has been previously proposed for giving alternative expressions [1, 2] of the Mayadas–Shatzkes equations [3].

Since the validity of the Mayadas–Shatzkes equations is not firmly established in some cases [2, 4, 5] and since some limiting forms of the conductivity equations obtained in the framework of multidimensional conduction models [2] can be regarded [6] as alternative expressions of the Fuchs–Sondheimer function [7] (when the grain size takes infinite values), we attempt in this short paper to give an insight into the validity of the effective-relaxation-time procedure in the framework of a multidimensional model.

2. The effective-relaxation-time multidimensional model

2.1. Defining the effective-relaxation-time

An effective relaxation time τ_{eff} is used for representing the effects of electronic scattering from sources other than grain boundaries, i.e. the background and external-surface scatterings [1, 2]. The effects of scattering at grain boundaries is represented by a grain-boundary relaxation time, τ_{gb} [8].

As usual [2], the resultant relaxation time τ_r, is defined from the partial relaxation times by the following relation:

$$\tau_r^{-1} = \tau_{eff}^{-1} + \tau_{gb}^{-1} \quad (1)$$

An alternative form is

$$\tau_r^{-1} = \tau_{eff}^{-1}(1 + \tau_{eff}\tau_{gb}^{-1}) \quad (2)$$

Since the electrical conductivity is proportional to the relaxation time, provided that it does not depend on coordinates [2], an effective relaxation time, independent of the geometrical parameters of the films, may be defined from the relation

$$\sigma_{FS}/\sigma_0 \approx \tau_{eff}/\tau_0 \quad (3)$$

where σ_0 is the bulk conductivity, τ_0 the electron relaxation time in the bulk material and σ_{FS} the conductivity of a thin film exhibiting Fuchs–Sondheimer size effect [2, 7].

An analytical expression for σ_{FS}/σ_0, much simpler than the Fuchs–Sondheimer function [7], has been recently proposed [6]:

$$\sigma_{FS}/\sigma_0 = A_{FS}(\mu) \quad (4)$$

with

$$\mu = d\lambda_0^{-1}(1 + p)[2(1 - p)]^{-1} \quad (5)$$

$$A_{FS}(\mu) = \tfrac{3}{2}\mu[\mu - \tfrac{1}{2} + (1 - \mu^2)\ln(1 + \mu^{-1})] \quad (6)$$

where d is the film thickness, λ_0 the bulk mean free path and p the usual specular electron reflection coefficient at the film surface [2, 7].

2.2. Expression for the film conductivity

The expression for the film conductivity, σ_f, is then obtained from the general relation [2, 7]

$$\sigma_f/\sigma_0 = \frac{3}{4}\int_0^{\pi} d\theta\, \tau_r\tau_0^{-1} \sin^3\theta \quad (7)$$

By introducing Equation 2, Equation 7 becomes

$$\sigma_f/\sigma_0 \approx \tfrac{3}{4}(\tau_{eff}/\tau_0)\int_0^{\pi} d\theta(1 + \tau_{eff}\tau_{gb}^{-1})^{-1} \sin^3\theta \quad (8)$$

Previous calculations [9] have given the analytical solution of Equation 7 in the case where only grain-boundary scattering is operative, i.e. for

$$\tau_r^{-1} = \tau_{gb}^{-1} + \tau_0^{-1} \quad (9)$$

and

$$\sigma_{gb}/\sigma_0 = \frac{3}{4}\int_0^{\pi} d\theta(1 + \tau_0\tau_{gb}^{-1})^{-1} \sin^3\theta \quad (10)$$

0022–2461/88 $03.00 + .12

$$\sigma_{gb}/\sigma_0 = A_{gb}(\nu) \quad (11)$$

with [10]

$$\nu = D_g\lambda_0^{-1}(1 + t)[2(1 - t)]^{-1} \quad (12)$$

$$A_{gb}(\nu) = \frac{3\nu}{2C_1}\left\{\frac{\nu + C^2}{C_1} - \frac{1}{2} + \left[1 - \left(\frac{\nu + C^2}{C_1}\right)^2\right] \times \ln\left(1 + \frac{C_1}{\nu + C^2}\right)\right\} \quad (13)$$

where D_g is the average grain size and t the statistical transmission coefficient at the grain boundary, and

$$C_1 = 1 - C \quad (14a)$$

for polycrystalline films [2, 11]

$$C_1 = -C \quad (14b)$$

for columnar films [11] with $C = 4/\pi$.

From comparing Equations 3, 8 and 10, it is clear that

$$\sigma_f \approx \sigma_{FS}A_{gb}(\nu\sigma_0/\sigma_{FS}) \quad (15)$$

Introducing

$$\nu_{FS} = \nu\sigma_0/\sigma_{FS} \quad (16)$$

Equation 15 takes the general form of an effective-mean-free-path equation [1, 2]:

$$\sigma_f \approx \sigma_{FS}A_{gb}(\nu_{FS}) \approx \sigma_{FS}\sigma_{gb}\nu_{FS}/\sigma_0 \quad (17)$$

whose asymmetric form is

$$\frac{\sigma_f}{\sigma_0} \approx \left(\frac{\sigma_{FS}}{\sigma_0}\right)\left(\frac{\sigma_{gb}\nu_{FS}}{\sigma_0}\right) \quad (17a)$$

2.3. Numerical data

Numerical solutions to Equation 15 have been computed and compared with those derived from the following exact equation [12] obtained in the framework of the multidimensional model:

$$\sigma_f/\sigma_0 = A(b, \gamma) \quad (18)$$

with

$$b = \mu^{-1} + C_1\nu^{-1} \quad (19)$$

$$\gamma = b^{-1}(1 + C^2\nu^{-1}) \quad (20)$$

$$C = 4/\pi \quad (21)$$

C_1, μ and ν have been defined above (Equations 5, 12, 14a and 8b); then

$$A(b, \gamma) = \frac{3}{2b}[\gamma - \tfrac{1}{2} + (1 - \gamma^2)\ln(1 + \gamma^{-1})]$$

As shown in Tables I and II for polycrystalline and columnar films, respectively, for a given value of ν the relative deviation of the approximate equation (Equation 17) from the exact one (Equation 18) is less than 10% when μ takes values larger than a minimum value of μ, μ_{min}; the variations of μ_{min} with ν are given respectively for polycrystalline and columnar film in Figs 1a and b (Curves 1).

3. Practical point of view

3.1. Comparison between approximate expressions of Equation 18

Previous theoretical studies [13] have proposed the following approximate equation:

$$A(b, \gamma) \approx (b\gamma + C_2 b)^{-1} \quad (22)$$

with

$$C_2 = 0.375 \quad (22a)$$

provided that

$$\gamma \geqslant 0.4 \quad (23)$$

From Equations 19 and 20 this limiting condition becomes

$$\mu \geqslant \left[2.5\left(1 + \frac{C^2}{\nu}\right) - \frac{C_1}{\nu}\right]^{-1} \quad (23a)$$

Hence, for a given value of ν, μ must be larger than a minimum value μ_m whose variations with ν are drawn for a polycrystalline film in Fig. 1a (Curve 2) and for a columnar film in Fig. 1b (Curve 3).

TABLE I Relative deviation (%) of the approximate equation (Equation 17) from the exact one (Equation 18), in the case of polycrystalline structure

μ	ν						
	10	5	2	1.5	1	0.5	0.1
0.01	10.807	6.523	10.995	13.601	17.948	26.350	36.824
0.03	3.442	4.965	10.125	12.288	15.562	20.702	19.568
0.05	2.936	4.539	9.085	10.859	13.399	16.748	13.026
0.07	2.312	4.207	8.184	9.672	11.698	13.975	9.587
0.09	2.219	3.872	7.422	8.693	10.345	11.930	7.479
0.10	2.107	3.731	7.087	8.266	9.768	11.097	6.707
0.30	1.210	2.066	3.539	3.941	4.314	4.208	1.845
0.50	0.805	1.366	2.230	2.432	2.576	2.365	0.934
0.70	0.607	0.994	1.573	1.694	1.760	1.563	0.585
0.90	0.469	0.766	1.189	1.270	1.302	1.131	0.409
1.00	0.424	0.684	1.052	1.121	1.144	0.985	0.352
3.00	0.120	0.189	0.273	0.283	0.279	0.226	0.074
5.00	0.065	0.102	0.146	0.205	0.145	0.117	0.038
7.00	0.049	0.069	0.341	0.093	0.097	0.077	0.025
9.00	0.036	0.050	0.059	0.074	0.072	0.057	0.018
10.0	0.030	0.044	0.061	0.064	0.063	0.050	0.016
30.0	0.021	0.006	0.019	0.019	0.019	0.015	0.005
50.0	0.010	0.013	0.015	0.015	0.014	0.010	0.003
70.0	0.050	0.002	0.004	0.005	0.005	0.004	0.001
90.0	0.027	0.016	0.008	0.006	0.004	0.002	0.000

TABLE II Relative deviation (%) of the approximate equation (Equation 17) from the exact one (Equation 18), in the case of columnar film

μ	ν						
	10	5	2	1.5	1	0.5	0.1
0.01	2.887	5.461	11.826	14.749	19.671	29.875	49.357
0.03	2.964	5.542	11.715	14.401	18.687	26.420	32.216
0.05	2.875	5.347	11.076	13.476	17.159	23.176	24.128
0.07	2.765	5.115	10.422	12.577	15.785	20.622	19.329
0.09	2.655	5.884	9.817	11.770	14.602	18.584	16.121
0.10	2.600	4.774	9.538	11.401	14.073	17.712	14.882
0.30	1.826	3.260	6.067	7.020	8.202	9.197	5.711
0.50	1.407	2.477	4.460	5.085	5.801	6.202	3.444
0.70	1.146	1.999	3.528	3.988	4.486	4.666	2.437
0.90	0.967	1.677	2.918	3.279	3.657	3.733	1.875
1.00	0.897	1.552	2.686	3.011	3.343	3.392	1.678
3.00	0.367	0.622	1.034	1.139	1.231	1.186	0.528
5.00	0.231	0.389	0.639	0.701	0.752	0.715	0.311
7.00	0.173	0.283	0.463	0.506	0.541	0.512	0.220
9.00	0.120	0.222	0.362	0.396	0.423	0.398	0.170
10.0	0.116	0.201	0.327	0.357	0.381	0.358	0.152
30.0	0.041	0.068	0.111	0.121	0.128	0.119	0.050
50.0	0.031	0.046	0.071	0.076	0.080	0.074	0.030
70.0	0.012	0.023	0.043	0.047	0.051	0.048	0.020
90.0	0.009	0.001	0.020	0.025	0.030	0.031	0.014

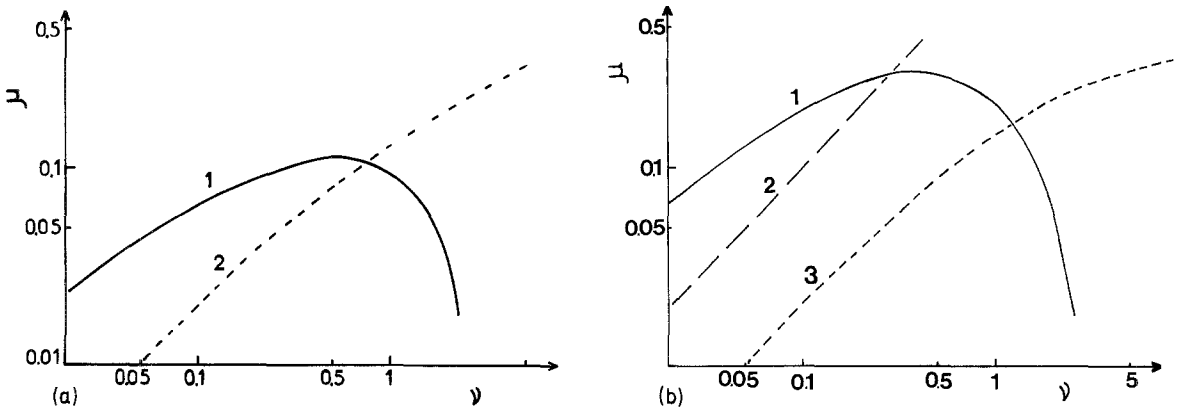

Figure 1 (a) Variations in μ with ν in the case of polycrystalline film: (1) variation in μ_{min} with ν, (2) variation in μ_m with ν. (b) Variations in μ with ν in the case of columnar structure: (1) variations in μ_{min} with ν, (2) $\mu = \nu$, (3) variations in μ_m with ν.

From Figs 1a and b it can be concluded that the effective-mean-free-path model is convenient when the grain boundaries do not act as efficient scatterers. In this case Equation 22 may be conveniently used.

3.2. Expression for the temperature coefficient of resistivity and the Hall coefficient

The temperature coefficient of resistivity (TCR), β_f, is defined as usual by

$$\beta_f = -\frac{d(\ln \sigma_f)}{dT} \tag{24}$$

where T is the absolute temperature.

In a similar way β_{FS} and β_{gb} can be defined from Equations 4 and 11 to give

$$\beta_{FS}(\mu) = \beta_0\left(1 - \frac{\partial \ln [A_{FS}(\mu)]}{\partial \ln \mu}\right) \tag{25}$$

$$\beta_{gb}(\nu) = \beta_0\left(1 - \frac{\partial \ln [A_{gb}(\nu)]}{\partial \ln \nu}\right) \tag{26}$$

A logarithmic differentiation of Equation 17 gives

$$\beta_f - \beta_{FS} \approx -\frac{\partial \ln [A_{gb}(\nu_{FS})]}{\partial \ln \nu_{FS}} \frac{\partial \ln \nu_{FS}}{\partial T} \tag{27}$$

where, from Equation 16,

$$\frac{\partial \ln \nu_{FS}}{\partial T} = \frac{\partial \ln \nu}{\partial T} + \frac{\partial \ln \sigma_0}{\partial T} - \frac{\partial \ln \sigma_{FS}}{\partial T} \tag{28}$$

i.e.

$$\frac{\partial \ln \nu_{FS}}{\partial T} = \beta_{FS} \tag{28a}$$

Hence Equation 27 becomes

$$\beta_f \approx \frac{\beta_{gb}\nu_{FS}}{\beta_0}\beta_{FS} \tag{29}$$

The reduced Hall coefficient of the film, R_{Hf}/R_{Ho} (R_{Ho} is the Hall coefficient of the bulk material) can be expressed [14, 15] in terms of the product of the reduced reciprocal conductivity with the reduced TCR, i.e.

$$\frac{R_{Hf}}{R_{Ho}} = \frac{\beta_f}{\sigma_f}\frac{\sigma_0}{\beta_0} \tag{30}$$

Combining Equations 17 and 29 gives

$$\frac{R_{Hf}}{R_{Ho}} \approx \frac{R_{Hf\text{-}FS}}{R_{Ho}}\frac{R_{Hf\text{-}gb}\nu_{FS}}{R_{Ho}} \tag{31}$$

where $R_{Hf\text{-}FS}$ is the Hall coefficient of a thin film in which no grain-boundary scattering occurs and $R_{Hf\text{-}gb}$ the Hall coefficient of an infinitely thick film in which grain-boundary scattering is operative.

3.3. Qualitative interpretations of the shifts in the Hall coefficient during the ageing procedure

3.3.1. Ordinary Hall coefficient of nickel film

Irreversible shifts in the ordinary Hall coefficient of thin nickel films, R_{Hf}, have been reported previously by De Groot [16] (Fig. 2); a recent reinterpretation of the electrical conduction and Hall effect in annealed films [17] has given evidence for the existence of a polycrystalline structure. Consequently the observed variations in R_{Hf} (Fig. 2) before and after annealing [16] can be described by Equation 31.

Since the ageing procedure induces an increase in the conductivity due to an increase in either λ_0 or p [18], an increase in the value of μ and a decrease in that of $R_{Hf\text{-}FS}$ can be predicted; on the other hand a decrease in ν_{FS}, at constant grain size, induces an increase in $R_{Hf\text{-}gb}$. Since the effect of the grain boundary does not modify markedly the Hall coefficient, except for very fine grains [12, 19, 20], the shift in R_{Hf} is mainly due to $R_{Hf\text{-}FS}$. It is consistent with the fact that Curves 1 and 2 in Fig. 2 may be made to coincide by changing the origin of the coordinates (Fig. 3).

Moreover Equation 31 gives a qualitative interpretation of the fact that the value of R_{Hf} depends on the deposition rate [16] since a variation in the average grain size is probable in this case, by analogy with the results related to other metals [21].

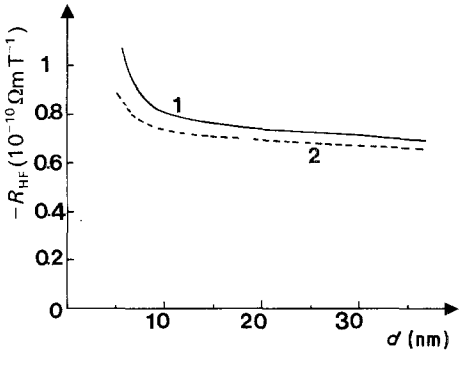

Figure 2 The variation of the ordinary Hall coefficient with thickness for nickel films (from De Groot [16]): (1) as-deposited films, (2) annealed films at 273 K.

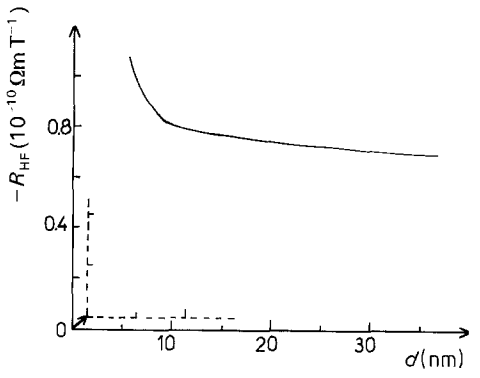

Figure 3 The shift in the coordinates allowing the coincidence of Curves 1 and 2 from Fig. 2.

3.3.2. Ordinary Hall coefficient of Ni–P films

In the case of chemically deposited Ni–P layers annealed at temperatures varying from 100 to 400° C, Viard [22] observed variations in the ordinary Hall coefficient, R_0, which depend markedly on the film thickness and annealing temperature (Fig. 4). In the case of films annealed at 400° C, which exhibit a crystalline structure [23], a marked size effect in R_0 occurs at very low thickness whereas it occurs for much larger values of thickness in the case of incompletely crystallized layers.

A general study [24] has shown that the size effect in the Hall coefficient can be represented (at its first step) by the approximate expression

$$R_{Hf}/R_{Ho} \approx 1 + 0.06\gamma^{-2} \quad (32)$$

Hence

$$R_{Hf-FS}/R_{Ho} \approx 1 + 0.06\mu^{-2} \quad (33)$$

and

$$\frac{R_{Hf-gb}}{R_{Ho}} \approx 1 + 0.06\left(\frac{\nu + C^2}{C_1}\right)^{-2} \quad (34)$$

Since the experimental variations in R_{Hf} with thickness roughly satisfy Equation 33 (Fig. 5) it can be concluded that the grain boundaries do not act as efficient scatterers. Hence, from Equation 17 it can be predicted that the size effect is mainly determined by R_{Hf-FS} and is therefore slightly modified by the ageing

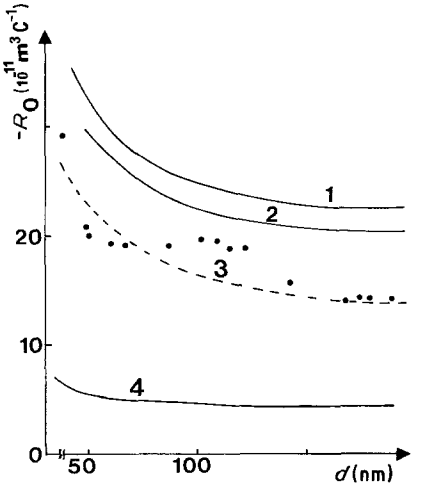

Figure 4 The variations in the ordinary Hall coefficient of Ni–P layers with the thickness for different annealing temperature (from Viard [22]): (1) 100° C, (2) 200° C, (3) 300° C, (4) 400° C.

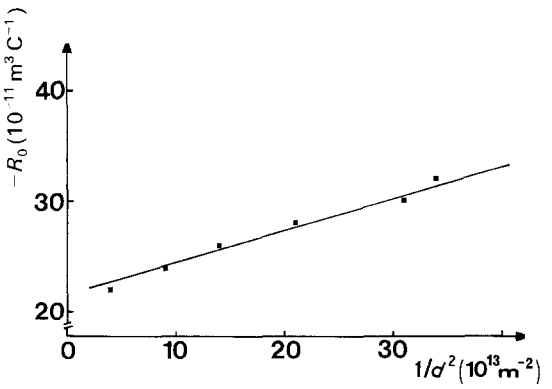

Figure 5 The variations of the ordinary Hall coefficient of Ni–P layers with the reciprocal square of the thickness (from Curve 1 of Fig. 4).

temperature (from 100 to 300° C), in good agreement with experiments (Fig. 4).

4. Conclusion

The effective-relaxation-time multidimensional conduction model can be regarded as a convenient tool for separating the effects of the ageing procedure on the surface and grain-boundary scatterings. Moreover it gives an insight into the evolution of the Hall coefficient when thermal treatments are operative.

References

1. C. R. TELLIER, *Electrocomp. Sci. Technol.* **5** (1978) 127.
2. C. R. TELLIER and A. J. TOSSER, "Size Effects in Thin Films" (Elsevier, Amsterdam, 1982) Ch. 1.
3. A. F. MAYADAS and M. SHATZKES, *Phys. Rev. B* **1** (1970) 1382.
4. C. R. PICHARD, M. BEDDA and A. J. TOSSER, *J. Mater. Sci. Lett.* **3** (1984) 725.
5. C. R. PICHARD, M. BEDDA, Z. BOUHALA, L. OUARBYA and A. J. TOSSER, *J. Mater. Sci.* **20** (1985) 867.
6. C. R. PICHARD, M. BEDDA, V. I. VATAMANYUK, A. J. TOSSER and C. R. TELLIER, *ibid.* **20** (1985) 4185.
7. E. H. SONDHEIMER, *Adv. Phys.* **1** (1952) 1.
8. C. R. TELLIER, *Thin Solid Films* **51** (1978) 311.
9. C. R. TELLIER, C. R. PICHARD and A. J. TOSSER, *ibid.* **61** (1979) 349.
10. M. BEDDA, S. MESSAADI, C. R. PICHARD and A. J. TOSSER, *J. Mater. Sci.* **21** (1986) 2643.
11. C. R. PICHARD, V. I. VATAMANYUK, A. KHALID-NACIRI, C. R. TELLIER and A. J. TOSSER, *J. Mater. Sci. Lett.* **3** (1984) 447.
12. V. I. VATAMANYUK, A. J. TOSSER, C. R. PICHARD and C. R. TELLIER, *J. Mater. Sci.* **19** (1984) 4138.
13. M. BEDDA, C. R. PICHARD and A. J. TOSSER, *ibid.* **21** (1986) 1405.
14. C. R. PICHARD, C. R. TELLIER and A. J. TOSSER, *ibid.* **1** (1982) 423.
15. A. J. TOSSER, C. R. PICHARD, M. LAHRICHI and M. BEDDA, *J. Mater. Sci. Lett.* **4** (1985) 585.
16. P. M. De GROOT, PhD thesis, Technical University of München, FRG (1980).
17. C. R. PICHARD, M. BEDDA, M. LAHRICHI and A. J. TOSSER, *J. Mater. Sci.* **21** (1986) 469.
18. K. L. CHOPRA, "Thin Film Phenomena" (McGraw-Hill, New York, 1969) Ch. VI.
19. C. R. PICHARD, A. J. TOSSER and C. R. TELLIER, *J. Mater. Sci.* **16** (1981) 451.
20. C. R. TELLIER and A. J. TOSSER, "Size Effects in Thin Films" (Elsevier, 1982) Ch. 2.

21. K. L. CHOPRA, "Thin Film Phenomena" (McGraw-Hill, New York, 1969) Ch. IV.
22. M. VIARD, PhD thesis, Université de Nancy 1 (1974).
23. F. MACHIZAUD, PhD thesis, Université de Nancy 1 (1973).
24. C. R. PICHARD, A. J. TOSSER and C. R. TELLIER, *J. Mater. Sci. Lett.* **1** (1982) 260.

Received 23 March
and accepted 8 June 1987